

# Impact of Nanoparticles Shape and Dye Property on the Photocatalytic Degradation Activity of TiO<sub>2</sub>

Elvis Fosso-Kankeu<sup>1</sup>, Frans Waanders<sup>2</sup>, Maryka Geldenhuys<sup>3</sup>

School of Chemical and Minerals Engineering, Faculty of Engineering, North-West University, South Africa

**Abstract:** Chemical and physical treatments of commercial titanium dioxide (TiO<sub>2</sub>) was carried out in this study to generate the shapes suitable for the photocatalytic degradation of Methyl Orange (MO), Congo Red and Methylene Blue which are anionic and cationic dyes respectively. The synthesized TiO<sub>2</sub> was characterized using scanning electron microscopy (SEM), X-ray diffractometer (XRD) and Fourier transform infrared spectroscopy (FTIR) and then used under simulated sunlight for the degradation of dyes. The SEM results showed that smaller particles of TiO<sub>2</sub> were formed after heating while the chemical treatment resulted in the formation of square-like particles. The XRD results showed that treatments resulted in the dominance of anatase phase and occurrence of the brookite phase. Various concentrations of dyes were considered to assess the photocatalytic degradation capacity and adsorption behaviour of TiO<sub>2</sub>. The experiments were carried out in a lightproof chamber with a 92.4% simulation of sunlight. It was found that up to 60% more degradation takes place in cationic dyes than anionic dyes, because of higher adsorption preceding the degradation. A small particle with a high anatase phase is also more effective for most dyes than other particles under sunlight like conditions. Thus the commercial TiO<sub>2</sub> is the most effective TiO<sub>2</sub> particle to use for photocatalytic degradation under sunlight like conditions.

**Keywords:** Photocatalytic degradation, sunlight conditions, TiO<sub>2</sub>, nanoparticle phase, anionic dye, cationic dye

## 1. Introduction

Dyes are among the main pollutants of fresh drinking water; an important aspect of water purification will therefore consist of the degradation of dyes in solution. Dyes are used in almost every sector of the industry, for example dyes are found in clothing, food colouring, yarn, leather, and even in the microbiology sector for staining. There are more than 100,000 types of dye available commercially [1-4]. Although care is taken to dispose of dyes correctly, some effluents are washed into the water system; this is a big environmental concern for water treatment since dye is difficult to remove, not readily biodegradable and even a small amount (1 mg/L) can affect water aesthetically [5-8]. Methods used to remove dyes from solution include adsorption of the dye by a material or flocculants and degradation of the dye by an oxidising component. The degradation of an azo dye poses a challenge since it has noxious aromatic immediate formation, which can be converted to carcinogenic compounds [9].

A lot of research has been focusing on the utilisation photocatalysis to degrade dyes in water, particles with oxidising capabilities are among the effective methods for dye removal; the particle method can be activated by photocatalysis to improve the degrading of the dyes, many forms of oxidising components have been tested [10-17]. Synthesis of gold, zinc, silver and other metallic compounds with an oxidising compound such as ZnO and TiO<sub>2</sub> particles have been extensively researched to determine the effectiveness (usefulness) of the particles as well as their efficiency for the degradation of dyes [18]. For the improvement of degradation and recovery, some metal oxides are doped with other metals such as gold, silver and iron [18]. To improve safety for human consumption, some of these particles are immobilized in a cloth or solid structure [19, 20]. TiO<sub>2</sub> is the chosen material for most of these studies as it is one of the most stable and non-toxic materials with photocatalytic capabilities available to the

industry [21]. TiO<sub>2</sub> is used as a whitening agent in toothpaste as well as a white food colouring and is thus not harmful for human consumption; it is also commercially available and can be used in various forms, shapes and sizes [22]. The efficiency of TiO<sub>2</sub> in photocatalysis of dyes has been tested on certain dyes within different conditions; during research, different shapes of TiO<sub>2</sub> nanoparticles are synthesized with different reaction conditions, reagents and additives. A few of the shapes of TiO<sub>2</sub> have been compared with each other for their efficiency in photocatalysis, it has been concluded that the use of smaller particles is the most effective for photocatalysis as the increased surface area improves the reaction capability [22]. Because scattering of light and a larger surface area can enlarge light harvesting, mesoporous nanoparticles could perform better than conventional anatase phase TiO<sub>2</sub>; however some shapes have been found to be less efficient than commercially available Degussa p25, which is a combination of rutile and anatase phases of TiO<sub>2</sub> [6]. It has been found that the capacity of degradation can be influenced by the shape of the nanoparticles. The synthesis for shape controlled nanoparticles has been successful in several cases [23]. In the study of Liao and Liao [24], who investigated the effect of the physical properties on the photocatalytic activity of TiO<sub>2</sub>, it was found that shape-controlled nanoparticles perform better than nanoparticles produced without surfactants; the cubic shaped nanoparticle is found to be superior in this regard. The production of small particles provides larger surface area enhancing the performance of nanoparticles; in the study, the uniformity of the shape was shown through Scanning Electron Microscope (SEM) images [24].

Many methods exist for creating nanoparticles; some of the popular methods include the Sol-Gel method, a precursor for TiO<sub>2</sub> is dissolved in water or ethanol and if shape- and size controlling is required a surfactant is added to the mixture [24]; this results into a mixture which is dried under prescribed conditions to form a gel. The Sol-Gel method is a relatively easy method for synthesizing nanoparticles and uses less energy than most other methods since particles are

synthesized close to room temperature. Uniformity in shapes and size is a problem with the Sol-Gel method; advancements in this area have been achieved by calcinating the gel at a temperature between 200-900 degrees Celsius to ensure uniformity [6].

Another method used in the creation of nanoparticles is the hydrothermal method[25]; in this method a precursor is mixed with acid and water, the reaction then takes place between 120 to 500 degrees Celsius for long periods of time, ranging from 6 to 120 hours[25].

The hydrothermal method is very energy and time consuming but produces relatively uniform results. In the microwave method a precursor is mixed with water, ethanol and chloroform, and is microwaved for 30 min at approximately 110 degrees Celsius [26]; this method is less energy and time consuming than the hydrothermal method and also produces relatively uniform results. Some other methods exist; one of these is the ultrasonic method, in which a sol-gel is optimised by ultrasonic waves [27]; the applied energy causes faster reaction since the change in energy is rapid. Doping of nanoparticles has also been considered and researched to find more efficient particles for photo catalysis; some particles are doped with iron to produce magnetic particles that can be recovered and reused.

The susceptibility of different dyes to photocatalytic degradation has been previously investigated, but the studies lack comparison of different shapes of nanoparticles, different shapes have been compared with only one azo dye[24]. Thus this study, aiming to compare the influence of shapes on the susceptibility of different azo dyes to photocatalytic degradation, will provide a fuller picture and a better understanding of the degradation of these dyes as well as the photocatalytic abilities of the different shapes and how they relate to one another.

## 2. Methodology

### Materials

Commercial TiO<sub>2</sub> and synthesized shapes were used for this study. The commercial TiO<sub>2</sub> and precursor as well as surfactants for the synthesized shapes were bought from Sigmateck and ACE. No further purification was required of these chemicals. The dyes used for this investigation was Methylene Blue (MB), Methyl Orange (MO) and Congo Red (CR). The most effective wavelengths were obtained by a wavelength search on the spectrophotometer and these wavelengths were used to calibrate the Spectrophotometer to determine adsorption and photocatalytic degradation of the dye.

### a) Synthesis of Nanoparticles

A square like shape was synthesized by using Titanium Butoxide as precursor. The molar ratios for the synthesis were used from Liao and Liao[24]. SDS was added as surfactant with ethanol as solvent. The solvent and precursor were mixed. The surfactant was slowly added with water as the limiting reagent to start the hydrolysis. The particles were then dried and calcinated at 600 degrees with an overshoot of 800 degrees Celsius.

### b) Characterization of the Nanoparticles

The shape and size of the nanoparticles was determined by SEM photographs from a TECSAN, model VEGA 3 XMU from Czech Republic, with 10 micron lens. XRD analysis was used to determine the composition of the particles; the diffractometer used was the Philips model X'Pert pro MPD, at a power of 1.6 kW used at 40 kV; Programmable divergence and anti-scatter slits; primary Soller slits: 0.04 Rad; 2θ range: 4-79.98; step size: 0.017°. FTIR analysis was done to define the adsorption affinity of each dye to each of the particles. The FTIR was a Shimadzu IRAffinity-1S, with a spectral range of 4000-400 cm<sup>-1</sup> with a resolution of 4 cm<sup>-1</sup>. These experiments were repeated twice for accuracy.

### c) Dye adsorption

The adsorption affinity of the dyes was determined by placing 0.05 g of nanoparticles in 100 mL of synthetic solution of the specific dye. This solution was then stirred at a constant speed in a light proof box for 9 min in the dark to determine the adsorption of the dye. Samples were drawn after 9 min, centrifuged and tested via a spectrophotometer for the determination of dye removal due to adsorption. These experiments were repeated three times and done in duplicate to minimize the errors.

### d) Dye degradation

The degradation of the dyes were determined in a batch type process after exposure for 9 min in the dark to separate the adsorption from the degradation process, 90 min of 92.4% strength of sunlight like conditions were considered for the degradation, with samples taken in specified times of 15 min, 30 min, 60 min and 90 min. These samples were centrifuged and the concentration of the remaining dye was determined by a spectrophotometer. The data obtained was then interpreted for the kinetic reaction rates for degradation. These experiments were repeated three times and done in duplicate to minimize the errors.

### e) Isotherm and kinetic models

The adsorption affinity of the dyes on the nanoparticles was determined by the Langmuir and Freundlich isotherms: The linear expression of the Langmuir model is as follow[28-31]:

$$\frac{C_e}{q_e} = \frac{1}{q_m k} + \frac{C_e}{q_m} \quad (1)$$

where:  $C_e$  is the dyes' equilibrium constant in (mg/L),  $q_e$  is the amount of adsorbed dye at equilibrium in (mg/g),  $Q_0$  is a Langmuir constant associated with the adsorption capacity in (mg/g),  $b$  is a Langmuir constant associated with the energy released during adsorption in (L/mg)

The linear expression of the Freundlich model is as follow [29, 30]:

$$\log q_e = \log k_f + \frac{1}{n} \log C_e \quad (2)$$

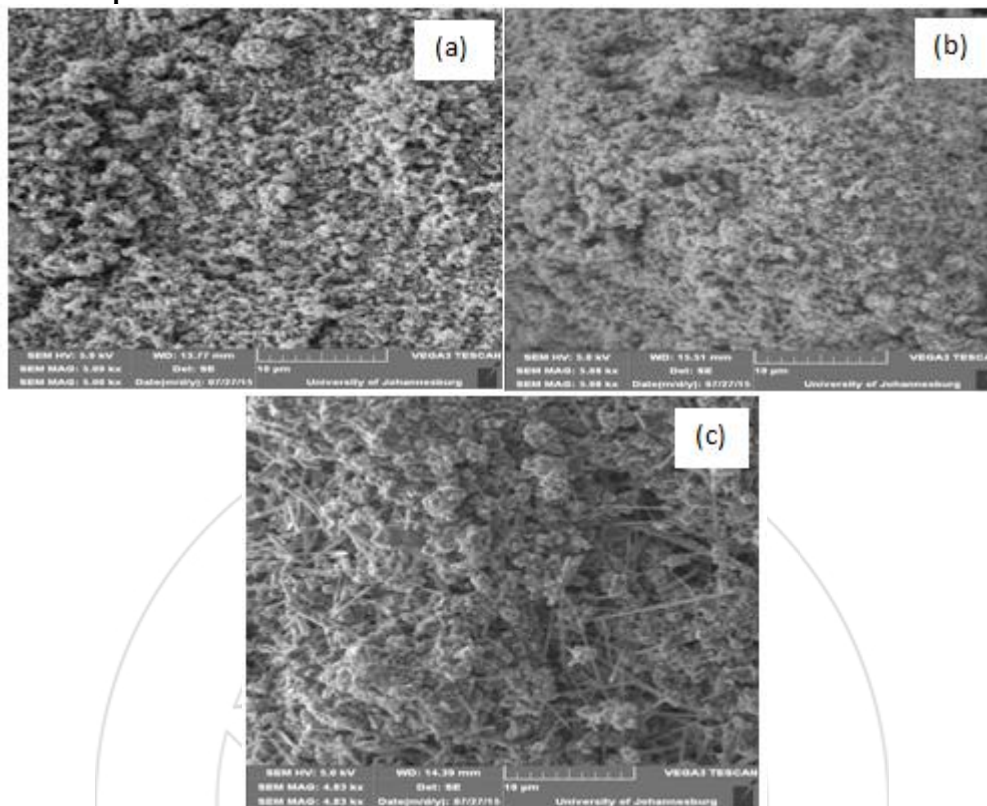
where:  $q_e$  is the concentration of the dye at equilibrium in its solid form (mg/g),  $C_e$  is the concentration of the dye at equilibrium in the solution (mg/L),  $k_f$  is the adsorption capacity measured (mg/g),  $n$  is the intensity of adsorption

The degradation rate was determined by plotting the amount degraded over time. The optimum amount degraded per hour

was considered to determine the state of nanoparticle the most suitable.

### 3. Results and discussion

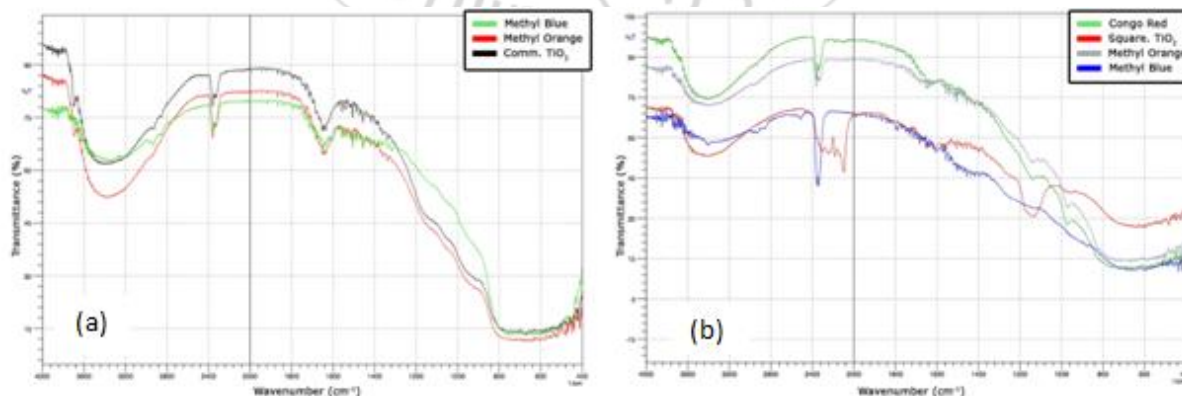
#### Characterization of nanoparticles



**Figure 1:** SEM images of (a) commercial TiO<sub>2</sub> (TiO<sub>2</sub>), (b) calcinated commercial TiO<sub>2</sub> (TiO<sub>2</sub>-Calc) and (c) square-like shaped TiO<sub>2</sub> (TiO<sub>2</sub>-Square)

It was observed (Fig. 1(b)) that the particle size of the calcinated TiO<sub>2</sub> was much smaller, in this case the nanoparticles shrunk a little bit because of the heat of calcination.

The synthesized TiO<sub>2</sub> (Fig. 1(c)) exhibited a heterogeneous shape and size; although the square like shape containing some few nanorods was observed, the cubic like shape was the most dominant. The FTIR analysis of pristine and dye loaded nanoparticles exhibited diverse spectra shown in Fig. 2(a), (b) and (c).



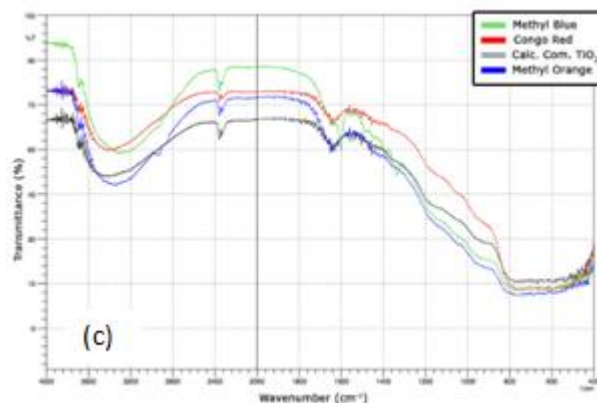


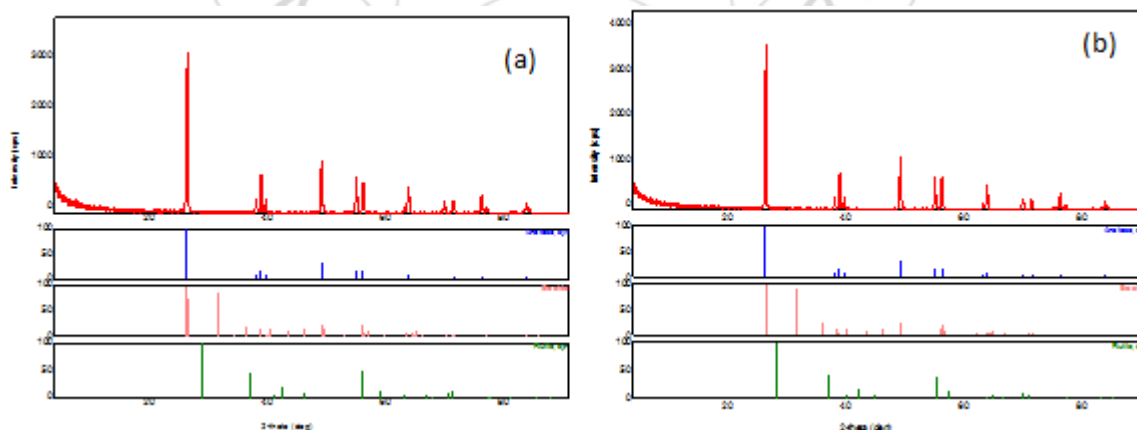
**Figure 2:** FTIR spectra of (a) pristine TiO<sub>2</sub> (black) and loaded with MB(green) and MO(red), (b), TiO<sub>2</sub>-Square (red) and TiO<sub>2</sub>-Square loaded with CR (green), MO (grey) and MB(blue), and (c) TiO<sub>2</sub>-Calc (grey) and TiO<sub>2</sub>-Calc loaded with MB(green), CR (red) and MO (blue)

The FTIR analysis shows two distinctive areas on each particle, which can be responsible of the adsorption taking place. From the figures it can be seen that the MB has more affinity to adsorbents than MO or CR. This can be ascribed to the electrostatic reaction between the charge of the different dyes and the nanoparticles. Methylene Blue is cationic in nature and can thus be easily adsorbed since the electrostatic interaction is more favourable, while MO and CR are anionic dyes, which adsorb less to the net negatively charged nanoparticles because of less favourable electrostatic interaction.

The Square like shape has peak (Fig. 2(b)) where it adsorbs all different dyes between 1000 and 1200 cm<sup>-1</sup>. This peak defined the tertiary amine groups that can be considered as binding groups, from the structures of the dyes this is a possible adsorption site. The TiO<sub>2</sub>-square nanoparticle loaded with MB does not exhibit a peak in this region, while the nanoparticle loaded with other dyes and the pristine nanoparticle showed two peaks in the region 980 – 1160 cm<sup>-1</sup>

due to the C – C and C – O symmetric stretching; the lack of peak in that region after exposure to MB clearly translate into the adsorption affinity for MB which is more favourable than the anionic dyes; this is further confirmed by the pronounced intensity of the peak at 2300 cm<sup>-1</sup> on the spectrum of MB loaded nanoparticle, this peak is characteristic of the CN stretch group from the dyes. The control and the loaded calcinated commercial nanoparticle (Fig. 2(c)) exhibited peaks between 1640 and 1700 cm<sup>-1</sup> as well as between 2000 and 2400 cm<sup>-1</sup>. The particularity of the TiO<sub>2</sub>-Calc loaded with MB was again observed as its spectrum exhibited a unique peak at 1600 cm<sup>-1</sup> indicating the C=C aromatic group deriving from the structure of MB. For the commercial TiO<sub>2</sub> (Fig. 2(a)) a shift of peak between 1640 and 1700 cm<sup>-1</sup> was likely due to the adsorption of MB.

XRD analysis of the nanoparticles allowed to obtain the following results (Fig. 3(a), (b) and (c)).



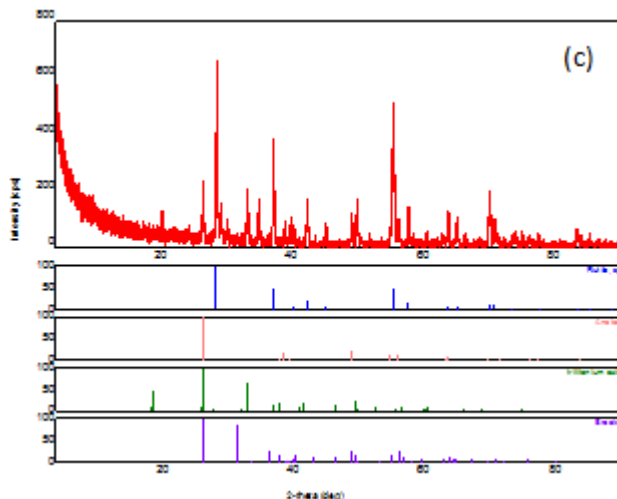


Figure 3: XRD results of (a) TiO<sub>2</sub>, (b) TiO<sub>2</sub>-Calc and (c) TiO<sub>2</sub>-Square

The XRD results exhibit the peaks representing anatase, rutile and or brookite phases in the nanoparticles, the calcination improved the amount of rutile phase in the particles. Anatase phase are more reactive photo-chemically and are thus favourable for photocatalytic degradation. Rutile phase have a larger eV gap than anatase phase and are suitable for water splitting. The mixing of phases were found to be more photocatalytic favourable than anatase phase with 0.14 eV electron gap higher than the anatase phase [27].

Anatase and brookite are meta stable while rutile is very thermodynamically stable and can be reached by high heat[32]. The results in Table 1 depict the percentage of the phases present in the particles.

Table 1: Percentage of Phases present in nanoparticles

Particles	Anatase	Rutile	Brookite	TiO <sub>2</sub>
Commercial	99.23	0.11	0.65	0
Calcinated	89.81	9.60	0.59	0
Square like	13.78	68.81	1.51	15.90

From Table 1 it is observed that the square like particle has

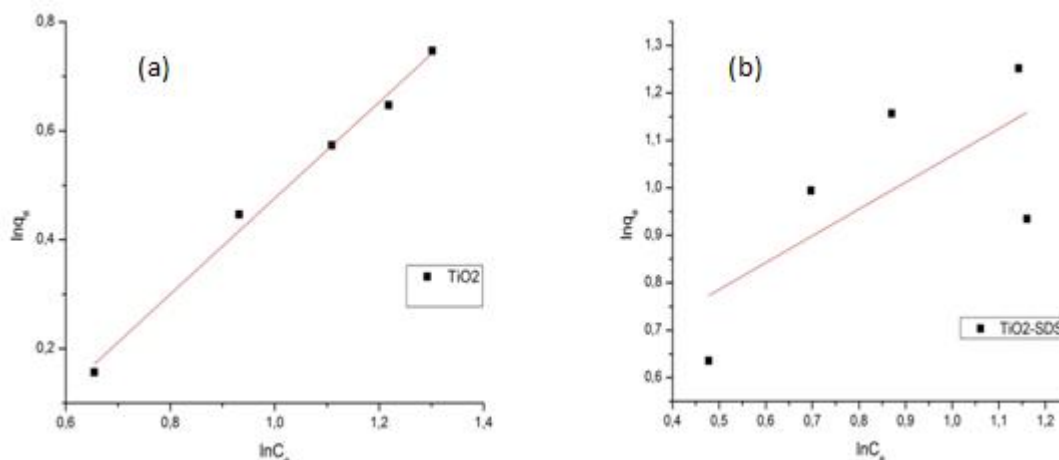


Figure 4: Freundlich isotherm data of adsorption equilibrium plot of (a) TiO<sub>2</sub> (A) and (b) TiO<sub>2</sub>-SDS for the removal of MB Dye

From Fig. 4(a) and (b), it can be observed that both TiO<sub>2</sub> and TiO<sub>2</sub>-SDS plots have a positive slope for the Freundlich

more rutile phase, while the commercial and the calcinated commercial are dominantly anatase phase. It is also seen that calcination improves the amount of rutile phase from the commercial particles. A mixture of phases is likely to induce more photocatalytic degradation, however the photocatalytic favourable anatase phase was found to be most effective.

#### 4. Adsorption behaviour of nanoparticles

The data were analysed using the Langmuir and Freundlich isotherm models to determine the adsorption behavior of the nanoparticles during the removal of dyes. The results show that the adsorption of MB by the commercial TiO<sub>2</sub> could be expressed better by the Freundlich isotherm model, while the Langmuir model did not fit the adsorption equilibrium data from any of the nanoparticles used. The linearized plot of log(qe) and log (Ce) for the adsorption of MB by the nanoparticles is shown in Fig. 4(a) and (b); the values of R<sup>2</sup> and Freundlich constants Kf and 1/n calculated from the intercept and slope of the plot are shown in Table 2.

model, but only the first has an R<sup>2</sup> value closer to unity, therefore implying a better fit. The slope and intercept of the

line with the y-axis were used to calculate the Freundlich isotherm parameters of the models. The calculated parameters are tabulated in Table 2:

**Table 2:** Freundlich isotherm model data

Nanoparticle	Parameters	MB	MO	CR
TiO <sub>2</sub>	R 2	0,9923	0,7556	0,6841
	1/n	0,8826	1,3286	0,9962
	K <sub>f</sub>	0,3922	0,0221	0,1653
TiO <sub>2</sub> -SDS	R 2	NF	NF	0,8039
	1/n			1,289
	K <sub>f</sub>			0,091
TiO <sub>2</sub> -Calc	R 2	NF	0,6420	0,6949
	1/n		1,8760	0,9701
	K <sub>f</sub>		0,2280	0,2627
TiO <sub>2</sub> -Square	R 2	NF	0,5005	0,7780
	1/n		1,3186	1,0330
	K <sub>f</sub>		0,0215	0,2978

NF: No fit

## 5. Degradation behaviour of nanoparticles

By plotting the amount of dye degraded against time, it was possible to determine the rate of degradation of dyes by the nanoparticles. The optimum time for the degradation was therefore determined from the graph. This allowed to plot the graphs of the degradation of 5 mg/L of dyes by the nanoparticles of different shapes.

Based on the Fig. 5(a), (b) and (c), MB is most susceptible to degradation when compared to the other dyes because of its natural loading onto the nanoparticles prior to the photocatalytic degradation process.

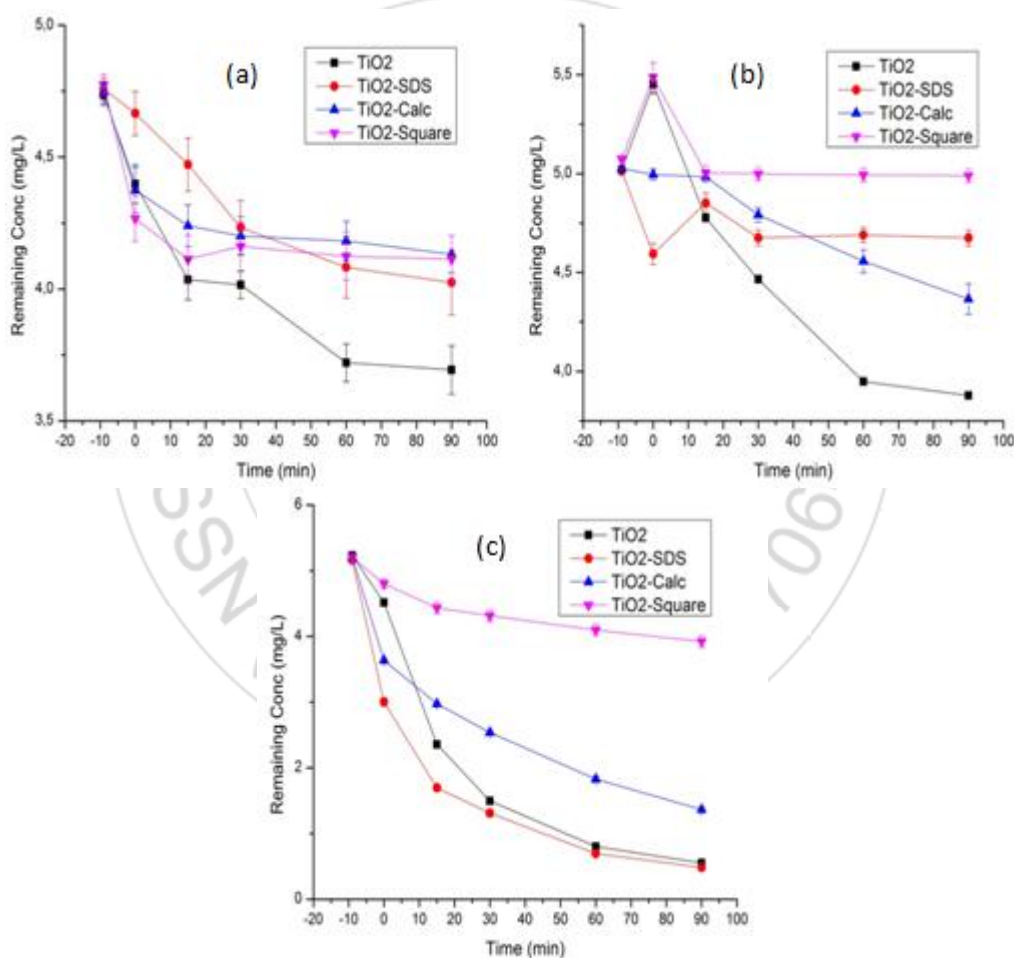


**Figure 5:** Amount of degradation graphs per amount of time for (a) CR, (b) MO and (c) MB

The figures show that MB is more likely to degrade, while lower degradation capacity was recorded for MO and CR due to their charge and the poor electrostatic interaction between the dyes and the nanoparticles.

The degradation rates of the nanoparticles at various concentrations of the dyes tested are shown in Table 3.

**Table 3:** Maximum degradation rate of dyes in the presence of nanoparticles

Nanoparticle	Degradation rate (mg/g/h)		
	Methylene Blue	Methyl Orange	Congo Red
TiO <sub>2</sub>	11.526	4.906	7.624
TiO <sub>2</sub> -SDS	20.346	3.506	6.134
TiO <sub>2</sub> -Calc	8.614	2.564	5.784
TiO <sub>2</sub> -Square	9.578	2.356	7.688

As shown on Fig. 5(a), (b) and (c), the adsorption affinity of the dye was the main factor that influenced the overall performance of the nanoparticles. Higher loading of dyes onto nanoparticles which results from adsorption, enhances the degradation capacity. Table 2 shows that the TiO<sub>2</sub>-SDS which exhibited better adsorption of MB was also the most effective nanoparticle during the degradation of MB; furthermore, the maximum degradation recorded by all the nanoparticles is achieved during the removal of MB. It can also be observed that to a certain extent, the performance of the nanoparticle is influenced by the nature of the dye as the TiO<sub>2</sub>-square performs better than the other nanoparticles during the degradation of CR. The commercial nanoparticle comparatively exhibits better degradation rate. It is however logical for the TiO<sub>2</sub> to exhibit better performance overall, due to larger surface area exhibited by its smaller particle size as well as the dominance of the most photocatalytic favourable phase in the nanoparticle, namely anatase phase.

## 6. Conclusion

The amount of dye degraded is influenced by the size and type of phase of the particle, the anatase phase also reported as favourable for photocatalytic degradation, was found to enhance the degradation of the dyes. The large surface area exhibited by smaller particle size was also found to be determinant for the photocatalytic degradation. The effect of particle's size and phase was evidenced as the commercial TiO<sub>2</sub> nanoparticle was the most effective in the degradation of the dyes. It was found that the dye affinity during adsorption also had a distinct effect on the overall performance as MB, which was effectively adsorbed, and could also be easily degraded than the other dyes. The overall best performance amongst all the nanoparticles was achieved by the commercial TiO<sub>2</sub> without any additives or calcination, this is likely due to its small size, the dominance of anatase phase, which is meta stable, and can react better than the rutile phase. Small particle size has larger surface area, which is crucial for the adsorption step that enhances the degradation rate. The additive SDS has the potential to improve adsorption, but only at high concentrations of cationic dyes. Thus for overall good performance the commercial TiO<sub>2</sub> nanoparticle should be considered.

## 7. Acknowledgements

The authors are grateful to the sponsor from the North-West University and the National Research Foundation (NRF) in South Africa. Any opinion, findings and conclusions or recommendations expressed in this material are those of the authors and therefore the NRF does not accept any liability in regard thereto. The contributions of Dr O. Ntwampe and Mr N. Lemmer from the North-West University and Mr E. Malenga and Ms N. Baloyi from the University of Johannesburg in South Africa are really appreciated.

## References

[1] Zollinger, H.: Color Chemistry: Synthesis, properties and applications of organic dyes and pigments, 2<sup>nd</sup> revised ed., VCH. (1991).

- [2] Konstantinou, I.K.; Albanis, T.A.: TiO<sub>2</sub>-assisted photocatalytic degradation of azo dyes in aqueous solution: kinetic and mechanistic investigations-A review. *Appl. Catal. B: Environ.* 49, 1-14 (2004).
- [3] Borker, P.; Salker, A.V.: Photocatalytic degradation of textile azo dye over C<sub>el-x</sub>Sn<sub>x</sub>O<sub>2</sub> series. *Mater. Sci. Eng. B.* 133 55-60 (2006).
- [4] Teng, T.T. and Louw, L.W.: Removal of Dyes and pigments from Industrial Effluents, In S.K. Sharma and R. Shangi, eds., *Advances in water treatment and pollution prevention*, 1st ed., Springer. pp. 65-93 (2002).
- [5] Prado, A.G.S.; Bolzon, L.B.; Pedroso, C.P.; Moura, A.O. and Costa, L.L.: Nb<sub>2</sub>O<sub>5</sub> as efficient and recyclable photocatalyst for indigo carmine degradation. *Appl. Catal. B: Environ.* 82 219-224 (2008).
- [6] Akpan, U.G.; Hameed, B.H.: Parameters affecting the photocatalytic degradation of dyes using TiO<sub>2</sub>-based photocatalysts: A review. *J. Hazard. Mater.* 170 520-529 (2009).
- [7] Mehra, M.; Sharma, T.R.: Photocatalytic degradation of two commercial dyes in aqueous phase using photocatalyst TiO<sub>2</sub>. *Adv. Appl. Sci. Res.* 3(2), 849-853 (2012).
- [8] Fosso-Kankeu, E.; Webster, A.; Ntwampe, I.O.; Waanders, F.B.: Coagulation/flocculation potential of polyaluminium chloride and bentonite clay tested in the removal of methyl red and crystal violet. *Ara. J. Sci. Eng.* DOI 10.1007/s13369-016-2244-x (2016).
- [9] Sreethawong, T.: Mesoporous-Assembled nanocrystal photocatalysts for degradation of azo dyes, In S.K. Sharma and R. Sangi, eds., *Advances in Water Treatment and Pollution Prevention*, 1<sup>st</sup> ed., Springer, India. pp. 147-175 (2012).
- [10] Chakrabarti, S.; Dutta, B.K.: Photocatalytic degradation of model textile dyes in wastewater using ZnO as semiconductor catalyst. *J. Hazard. Mater.* B112, 269-278 (2004).
- [11] Styliadi, M.; Kondarides, D.I. and Verykios, X.E.: Visible light-induced photocatalytic degradation of Acid Orange 7 in aqueous TiO<sub>2</sub> suspensions. *Appl. Catal. B: Environ.* 47, 189-201 (2004).
- [12] Su, C.; Hong, B.Y. and Tseng, C.M.: Sol-gel preparation and photocatalysis of titanium dioxide. *Catal. Today.* 96, 119-126 (2004).
- [13] Sun, J.; Wang, X.; Sun, J.; Sun, R.; Sun, S. and Qiao, L.: Photocatalytic degradation and kinetics of Orange G using nano-sized Sn(IV)/TiO<sub>2</sub>/AC photocatalyst. *J. Mol. Catal. A: Chem.* 260, 241-246 (2006).
- [14] Reddy, M.P.; Venugopal, A. and Subrahmanyam, M. (2007) Hydroxyapatite photocatalytic degradation of calmagite (an azo dye) in aqueous suspension. *Appl. Catal. B: Environ.* 69, 164-170 (2007).
- [15] Silva, C.G.; Wang, W. and Faria, J.L.: Photocatalytic and photochemical degradation of mono-, di- and tri-azo dyes in aqueous solution under UV irradiation. *J. Photochem. Photobiol. A: Chem.* 181, 314-324 (2006).
- [16] Sleiman, M.; Vildoza, D.; Ferronato, C. and Chovelon, J.-M.: (2007) Photocatalytic degradation of azo dye Metanil Yellow: optimization and kinetic modelling using a chemometric approach. *Appl. Catal. B: Environ.* 77, 1-11 (2007).

- [17] Saquiba, M.; Tariqa, M.A.; Faisala, M. and Muneer, M.: Photocatalytic degradation of two selected dye derivatives in aqueous suspensions of titanium dioxide. *Desalination*. 219, 301-311 (2008).
- [18] Rauf, M.A. and Ashraf, S.S.: Fundamental principles and application of heterogeneous photocatalytic degradation of dyes in solution. *Chem. Eng. J.* 151, 10-18 (2009).
- [19] Deneshvar, N.; Salari, D. and Khataee, A.R.: Photocatalytic degradation of azo dye acid red 14 in water on ZnO as an alternative catalyst for TiO<sub>2</sub>. *J. Photoch. Photobio. B.* 162, 317-322 (2004).
- [20] Geldenhuys, M.: Photocatalytic degradation of dyes with TiO<sub>2</sub> nanoparticles, BEng Report North-West University, Potchefstroom, South Africa, 2015.
- [21] Carp, O.; Huisman, C.L. and Reller, A.: Photoinduced reactivity of titanium oxide photoinduced reactivity of titanium oxide. *Solid State Chem.* 32, 33-177 (2004).
- [22] Sreethawong, T.: Mesoporous-Assembled nanocrystal photocatalysts for degradation of azo dyes, In S.K. Sharma and R. Sangi, eds., *Advances in Water Treatment and Pollution Prevention*, 1<sup>st</sup> ed., Springer, India. pp. 147-175 (2012).
- [23] Schneider, J.; Matsuoka, M.; Takeuchi, M.; Zang, J.; Horiuchi, Y.; Anpo, M. and Bahnemann, D.W.: Understanding TiO<sub>2</sub> photocatalysis: Mechanisms and Materials. *Chem. Rev.* 114, 9919-9986 (2014).
- [24] Liao, D.L. and Liao, B.Q. (2007) Shape, size and photocatalytic activity control. *J. Photoch. Photobio. A.* 187, 363-369 (2007).
- [25] Oh, J.-K.; Lee, J.-K., Kim, S.J. and Park, K.-W.: (2009) Synthesis of phase- and shape-controlled TiO<sub>2</sub> nanoparticles via hydrothermal process. *J. Ind. Eng. Chem.* 15, 270-274 (2009).
- [26] Wang, X.; Li, Z.; Shi, J. and Yu, Y.: One-dimensional Titanium Dioxide nanomaterials: Nanowires nanorods, and nanobelts. *Chem. Rev.* 114, 9346-9384 (2014).
- [27] Fosso-Kankeu, E.; Waanders, F. and Fraser, C.: Bentonite clay adsorption affinity for anionic and cationic dyes, *Proceedings of the 6<sup>th</sup> International Conference on Green Technology, Renewable Energy and Environmental Engineering (ICGTREEE'2014)*, Cape Town-South Africa, November 27-28, 2014, pp. 257-260 (2014).
- [28] Fosso-Kankeu, E.; Mulaba-Bafubiandi, A.F.; Mamba, B.B. and Barnard, T.G.: Prediction of metal-adsorption behaviour in the remediation of water contamination using indigenous microorganisms. *J. Env. Manage.* 92(10), 2786-2793 (2011).
- [29] Mittal, H.; Fosso-Kankeu, E.; Mishra, S.B. and Mishra, A.K.: (2013) Biosorption potential of Gum ghatti-g-poly (acrylic acid) and susceptibility to biodegradation by *B. subtilis*. *Int. J. Biol. Macromol.* 62, 370-378 (2013).
- [30] Fosso-Kankeu, E.; Mittal, H.; Mishra, S.B. and Mishra, A.K.: (2015) Gum ghatti and acrylic acid based biodegradable hydrogels for the effective adsorption of cationic dyes. *J. Ind. Eng. Chem.* 22, 171-178 (2015).
- [31] Fosso-Kankeu, E.; Mulaba-Bafubiandi, A.F.; Piater, L.A.; Tlou, M.G.: Cloning of the *cnr* operon into a strain of Bacillaceae bacterium for the development of a suitable biosorbent. *World J. Microb. Biot.* DOI 10.1007/s11274-016-2069-5 (2016).
- [32] Liu, G.; Yang, H.G.; Pan, J.; Yang, Y.Q.; Lu, G.Q. and Cheng, H.: (2014) Titanium Dioxide Crystals with tailored facets. *Chem. Rev.* 114, 9559-9612 (2014).